Feasibility study on a new pomelo peel derived biochar for tetracycline antibiotics removal in swine wastewater

Dongle Cheng[a], Huu Hao Ngo[a,b,e*], Wenshan Guo[a,b], Soon Woong Chang[c], Dinh Duc Nguyen[c,d], Xinbo Zhang[b], Sunita Varjani[f], Yi Liu[g]

[a]*Centre for Technology in Water and Wastewater, School of Civil and Environmental Engineering, University of Technology Sydney, Sydney, NWS 2007, Australia*
[b]*Joint Research Centre for Protective Infrastructure Technology and Environmental Green Bioprocess, Department of Environmental and Municipal Engineering, Tianjin Chengjian University, Tianjin 300384, China*
[c] *Department of Environmental Energy Engineering, Kyonggi University, 442-760, Republic of Korea*
[d]*Institution of Research and Development, Duy Tan University, Da Nang, Vietnam*
[e] *NTT Institute of Hi-Technology, Nguyen Tat Thanh University, Ho Chi Minh City, Vietnam*
[f] *Gujarat Pollution Control Board, Paryavaran Bhavan, CHH Road, Sector 10A, Gandhinagar – 382 010, Gujarat, India*
[g] *Department of Environmental Science and Engineering, Fudan University, 2205 Songhu Road, Shanghai 200438, PR China*

***** Corresponding authors: *E–mail address:* ngohuuhao121@gmail.com

Abstract

Removal of tetracycline antibiotics (TCs) by biochar adsorption is emerging as a cost-effective and environmentally friendly strategy. This study developed a novel pomelo peel derived biochar, which was prepared at 400 °C (BC-400) and 600 °C (BC-600) under nitrogen conditions. To enhance the adsorption capacity, BC-400 was further activated by KOH at 600 °C with a KOH: BC-400 ratio of 4:1. The activated biochar (BC-KOH) displayed a much larger surface area (2457.37 m^2/g) and total pore volume (1.14 cm^3/g) than BC-400 and BC-600. High adsorption capacity of BC-KOH was achieved for removing tetracycline (476.19 mg/g), oxytetracycline (407.5 mg/g) and chlortetracycline (555.56 mg/g) simultaneously at 313.15 K, which was comparable with other biochars derived from agricultural wastes reported previously. The adsorption data could be fitted by the pseudo-second-order kinetic model and Langmuir isotherm model successfully. The initial solution pH indicated the potential influence of TCs adsorption capacity on BC-KOH. These results suggest that pore filling, electrostatic interaction and π–π interactions between the adsorbent and adsorbate may constitute the main adsorption mechanism. BC-KOH can be used as a potential adsorbent for removing TCs from swine wastewater effectively, cheaply and in an environmentally friendly way.

Keywords: Pomelo peel; Tetracycline antibiotics; Biochar; Adsorption

1. Introduction

Tetracycline antibiotics (TCs), which comprise tetracycline (TC), oxytetracycline (OTC) and chlortetracycline (CTC), are one of the most extensively used antibiotics in swine production worldwide. They are considered to have advantages of high efficiency, low cost, and broad spectrum (Kim et al., 2013). Generally, antibiotics are not completely absorbed and metabolized by animals, and in fact around 70–90% of them added to their feed are excreted via urine and feces (Cheng et al., 2018b). Subsequently, large concentrations of TCs have

been detected in swine wastewater and the surface water adjacent to swine farms (Cheng et al., 2019). Residual antibiotics in swine wastewater have attracted much attention worldwide due to their adverse effects on human health and ecological security (Cheng et al., 2019). Apart from the toxicity of veterinary antibiotics to organisms, the long-term presence of antibiotics in the environment can trigger the development of antibiotic-resistant bacteria (ARB) and antibiotic-resistant genes (ARGs) (Martínez, 2008). It was reported that tetracycline-resistant genes occupied the largest percentage of more than one hundred classes of ARGs found in bacterial isolates found in various environments (Zhang et al., 2009). The widespread existence of tetracycline-resistant genes (tetM, tetO, and tetW) in swine wastewater and the environment adjacent to swine farms has been documented in other analyses (Liu et al., 2013).

Technologies including biological processes, advanced oxidation processes (AOPs), electrochemical oxidation and adsorption, have been extensively investigated for their potential to remove antibiotics from swine wastewater (Ben et al., 2011; Cheng et al., 2019; Miyata et al., 2011; Peng et al., 2016; Qiang et al., 2006; Wang et al., 2019). As reported previously, conventional biological treatment processes cannot remove residual antibiotics from swine wastewater completely. Antibiotics' toxic effect on microorganisms can also limit the performance of biological treatment processes (Cheng et al., 2018a). Applying AOPs to remove antibiotics from swine wastewater is quick and effective, while consuming large amounts of energy and chemical reagents that significantly raise operating costs. In addition, chemical reagents consumed in chemical methods can also cause secondary pollution in the natural environment. Adsorption is a promising and better choice for the removal of antibiotics from wastewater, due to its advantages of effectiveness, low cost, easy operation and the adsorption process does not produce intermediate products. Several adsorption materials have been investigated for removing antibiotics from aqueous solution, such as activated carbon, carbon nanotubes, natural clay materials, ion exchange materials, and biochar (BC) (Ahmed et al., 2015). Of these materials, BC derived from agricultural wastes has been the subject of

enormous research focus, because of its advantages of originating from a wide range of raw materials, low-cost preparation, being environmentally friendly and having adsorption properties (Ahmad et al., 2014; Enders et al., 2012). To date, BC has been used to adsorb antibiotics from wastewater very efficiently (Chen et al., 2019; Dai et al., 2019).

Fruit peels, generated in significant amounts, can be used as raw materials for conversion into biochar through pyrolysis instead of being disposed as waste through landfilling, open burning or composting. Greenhouse gases emission, such as carbon dioxide and methane, from conventional disposal of these wastes is an important issue for global warming. The conversion of such waste to reusable resources is an alternative method for waste management, which achieved net energy production and avoided greenhouse gas emissions. For instance, Sial et al. (2019) indicated that the greenhouse gas emission was significantly reduced by converting orange peels waste to biochar. Pomelo is a very popular fruit and is planted around the world. According to the report by Food and Agriculture Organization (FAO), the global production of grapefruit (including pomelos) was around 9.37 million metric tons in 2018. Pomelo peels which account for nearly 45% of the total weight, are generally treated as agricultural waste, which is not only a waste of resources but also harms the environment (Liang et al., 2014). Compared to most other citrus fruits, pomelo peels are deemed to be promising raw materials for BC production. In addition to their high output, the white floc layer of the pomelo peel contains cellulose and semi-fiber with three-dimensional network structures and various active functional groups, which make the pomelo peel a promising raw material of biochar adsorbent (Song et al., 2019; Zhang et al., 2020). Moreover, the adsorption ability of pomelo peel BC can be enhanced through chemical activation (Romero-Cano et al., 2017).

The surface area and pore size are two important characteristics of biochar, which influence its adsorption capacity to organic pollutants (Ahmed et al., 2017a; Cheng & Li,

2018). According to previous reports, the carbon having enough pore size was required to create adsorption sites in pores for organic matter (Zhang et al., 2014). However, the surface area and pore size of the originally generated biochar are limited, so further activations are required to increase their surface area and porosity. Thermal treatment and KOH activation are common methods for the production of porous biochar (Zhu et al., 2018). In the study, pomelo peel derived biochar was prepared and activated to explore the feasibility of removing TCs from swine wastewater. The characteristics of the produced biochar and the adsorption capacity for TCs were investigated. Moreover, adsorption kinetics and isotherm modes were applied to analyse the adsorption process between the biochar and TCs. Outcomes of initial antibiotic concentration and pH on the adsorption process were explored. In addition, the possible adsorption mechanism between the adsorbent and adsorbate was predicted.

2. Materials and methods

2.1 Materials

Pomelo peel wastes were washed with distilled water and dried in an oven at 80 °C for 24 h, and following this they were crushed into small pieces prior to use. The standards of tetracycline antibiotics (TCs), including tetracycline (TC), oxytetracycline (OTC) and chlortetracycline (CTC) were supplied by Sigma-Aldrich (Australia). Organic solvents, such as methanol, acetonitrile and formic acid that were used for the TCs stock solution preparation and mobile phase for detecting the quantities of TCs by Shimadzu LCMS-8060 triple quadrupole mass spectrometer, were also purchased from Sigma-Aldrich, Australia. The other chemicals utilized were of analytical grade, specifically NaOH, HCl and KOH.

2.2 Biochar preparation and modification

Prepared pomelo peels were pyrolyzed at 400 °C and 600 °C, respectively, for 2 h with a heating rate of 10 °C min^{-1} in a muffle furnace. The resulting sample was designated as BC-400 and BC-600. The BC-400 was mixed with KOH at a mass ratio of 1:4, followed by

carbonization at 600 °C for 2 h in a muffle furnace with a heating rate of 10 °C min^{-1}. Biochar obtained from this activation was designated as BC-KOH, which was washed with 35% HNO_3 for 24 h and washed with DI water until the pH value of the filtrate reaches 7.0 ± 0.2. Finally, the produced biochar was oven-dried at 80 °C for 24h. The particle sizes of BC-400, BC-600 and BC-KOH were sieved (<75 μm) for further use.

2.3 Biochar Characterization

Surface morphology and elemental compositions of the prepared biochar were investigated using a scanning electron microscopy (SEM) and an energy dispersive spectrometer (EDS) (Zeiss Evo-SEM). Renishaw inVia Raman spectrometer (Gloucestershire, UK) was used to analyse the Raman spectra of the produced biochar. The functional groups present in the biochar were determined by Fourier transform infrared (FTIR) spectrometer (Miracle-10, Shimadzu) in the 4000-400 cm^{-1} range. Brunauer-Emmett-Teller (BET) analyzer (Quantachrome Autosorb IQ, USA) was applied to determine the surface area and pore size distribution of the biochar via adsorption/desorption isotherm of nitrogen at 77 K. Before adsorption measurements were taken, degassing of the sample was conducted under vacuum at 473 K for 6 h. The surface charges of the materials at different pH values were analysed by a zeta potential analyzer (Malvern, Model ZEN3600) at the solution pH ranging from 1.0 to 10.0.

2.4 Sorption experiments

The sorption capacity of BC-400, BC-600 and BC-KOH was investigated through batch experiments for 48 h. 10 mg BC-400, BC-600 and 4 mg BC-KOH were added to glass bottles containing 50 ml TCs solutions with 10 mg/L of TCs (TC, OTC and CTC) at 295.15 K. The adsorption kinetics of TCs on BC-KOH was conducted in 100 ml glass bottles by adding 4 mg BC-KOH (80 mg/L) to 50 ml TCs solution with an initial TCs concentration of 10 and 40 mg/L, at 295.15 K. The adsorption isotherms were obtained by mixing 4 mg BC-KOH and 50 mL TCs solution with different initial TCs concentrations (5-50 mg/L) at 294.15, 303.15

and 313.15 K for 75 h. For the sorption capacity and kinetic experiments, samples were collected at different time intervals, while samples for the sorption isotherms study were collected once the equilibrium adsorption point had been reached. All the samples were filtered through a 0.2 μm filter before being subjected to analysis. Bottles for all the above experiments were shaken on a temperature controlled orbital shaker at 120 rpm at pH value of 7.0 ±0.5. The influence of initial solution pH on the adsorption of TCs (40 mg/L) onto biochar was established by varying the pH value from 1.5 to 10 through using 0.01 mol/L of NaOH and HCl solution, at 294.15 K for 75 h. The application of BC-KOH on the adsorption of TCs from synthetic swine wastewater was investigated. The main composition of synthetic swine wastewater is glucose, NH_4Cl, KH_2PO_4, $MgSO_4 \cdot 7H_2O$ and $CaCl_2 \cdot 2H_2O$ with the concentration of 2830 m/L), 446 mg/L, 132 mg/L, 54 mg/L and 4 mg/L, respectively. TCs were spiked into the wastewater with the concentration of 10 mg/L for each compound. The same concentration of BC-KOH (80 mg/L) was used for the adsorption at pH 7.0 ± 0.5 and 294.15 K for 75 h. Blank control samples (without biochar) were prepared for each experiment to subtract the loss of TCs during the adsorption process. All experiments were performed in duplicate and mean and standard deviation were calculated.

2.5 Data analysis and analytical methods

Concentrations of TCs in the solutions were determined by LC-MS/MS (LCMS-8060, Shimadzu). A Phenomenex C18 column (Luna, 3.0 × 100 mm, 3 μm) was used at 28 ºC. The mobile phase A and B for LC gradient was water and acetonitrile with 0.1% formic acid (V/V). The LC gradient was: 0.01-0.20 min 30% B; 0.20-7.0 min 95% B; 7.0–11 min 30% B. The flow rate was 0.4 mL/min and the injection volume was 1 μL. Mass spectrometer was operated in the multiple reaction monitoring (MRM) mode and electrospray positive ion mode (ESI+).

The amount of TCs adsorbed on biochar at time t (q_t, mg/g) and equilibrium (q_e, mg/g) was calculated by Eq. (1) and (2):

$$q_t = \frac{(C_0 - C_t) \times V}{m} \quad (1)$$

$$q_e = \frac{(C_0 - C_e) \times V}{m} \quad (2)$$

where C_0, C_t and C_e are the concentrations of TCs initial, at time t and equilibrium (mg/L); V is the volume of TCs solution (L); and m (g) is the amount of biochar used in study.

For this study, the following adsorption kinetic models, i.e. pseudo-first-order (PFO), pseudo-second-order (PSO), Elovich, liquid film diffusion (LFD) and intra-particle diffusion (IPD) (Eq. (3-7) were selected to assess the adsorption mechanisms between the interaction of the biochar and TCs. The equations and relevant parameters can be expressed as follows:

$$q_t = q_e(1 - \exp(-k_1 t)) \quad (3)$$

$$q_t = \frac{k_2 q_e^2 t}{1 + k_2 q_e t} \quad (4)$$

$$\frac{dq_t}{dt} = a \exp(-b q_t) \quad (5)$$

$$\ln\left(1 - \frac{q_t}{q_e}\right) = -k_{fd} t \quad (6)$$

$$q_t = k_i \sqrt{t} + C_i \quad (7)$$

where, q_t and q_e (mg/g) are the amount of TCs adsorbed at time t (min) and equilibrium; k_1 and k_2 are the rate constants of the pseudo-first-order and pseudo-second-order, respectively; a is the rate constant of chemisorption; b is the constant of the surface coverage; $1/b$ (mg/g) is related to the number of sites available for adsorption; k_{fd} is the constant of adsorption rate; k_i (mg·min$^{0.5}$/g) is intra-particle diffusion rate constant; and C_i is the intercept reflecting the extent of the boundary layer thickness.

Two classic adsorption models, Freundlich and Langmuir models, were utilized to fit the adsorption isotherms, which are written as follows (Eq. (8-9)):

$$q_e = K_F c_e^{1/n} \quad (8)$$

$$q_e = \frac{q_m K_L c_e}{1 + K_L c_L}, \; R_L = \frac{1}{1 + K_L c_L} \quad (9)$$

Where, q_e is the adsorption capacity (mg/g) at equilibrium time; c_e is the equilibrium concentration (mg/L) of TCs in solution; K_F ($mg^{(1-n)}L^n/g$) is Freundlich affinity coefficient indicating adsorption capacity; 1/n presents the adsorption intensity; q_m is the maximum adsorption capacity (mg/g); $c_L$is the lowest initial concentration (mg/L); K_L (L/mg) is the Langmuir sorption coefficient related to the bonding force of adsorption; and R_L is a dimensionless constant separation factor. The Langmuir isotherm model will be favored if the value of R_L is between 0 and 1.

3. Results and discussion

3.1 Characterization of biochar

The biochar yield derived from pomelo peel was 35.93% at 400 ℃ and 32.78% at 600℃, respectively (Table 1). Based on a previous review paper, the value is comparable with the yield of biochar produced from other raw materials (Yang et al., 2019b). Like previous reports, a slight decline in the biochar yield was observed by increasing the pyrolysis temperature, which is explained by the loss of volatiles and condensation of aliphatic compounds (Zhao et al., 2017). The high biochar yield is generally considered to be an important factor in practical applications.

Table 1. Physicochemical properties of biochars produced under different conditions.

Sample	C (wt %)	O (wt %)	Yield (%)	BET surface area (m^2/g)	Total pore volume (cm^3/g)
BC400	66.1	14.89	35.93	3.278	0.003
BC600	72.21	14.01	32.78	27.501	0.021
BC-KOH	86.18	11.81	31.65	2457.367	1.14

The analytical results of EDS indicated that carbon was a dominant element in the produced biochar from pomelo peel. By increasing the pyrolysis temperature and KOH

activation, the carbon content increased from 66.1% to 86.18% (by weight), while the oxygen content decreased (Table 1). The decrease of oxygen content indicated less oxygen-containing functional groups on the biochar surface, which can be proved by the FTIR analysis results. The FTIR peak of biochars produced in the present study is illustrated in Fig. 1(A), and the FTIR spectrum curve displays peaks at about 2348, 1560, 1372 and 1168 cm^{-1} for BC400 and 2348,1623, 1397,1006 863, 831 and 695 cm^{-1} for BC-600. The peak at around 2348 and 2320 cm^{-1} may belong to C ≡C or C ≡N. The peak at approximately 1560 and 1623 cm^{-1} indicates the presence of C=C or C=O stretching in aromatic groups, while the peak at around 1397 and 1372 cm^{-1} may relate to the methyl C-H bending vibration in alkanes and alkyl groups (Uchimiya et al., 2011). The presence of a peak at 1168 and 1064 cm^{-1} possibly contributes to C-O, C-O-C or C-C stretching modes, while peaks at 900-695 cm^{-1} may belong to aromatic C-H bending vibration (Komnitsas & Zaharaki, 2016). Yet, most of the peaks disappeared after KOH activation, which confirmed the finding that functional groups' reduction on the surface of biochar after alkaline modification occurred (Yang et al., 2019b).

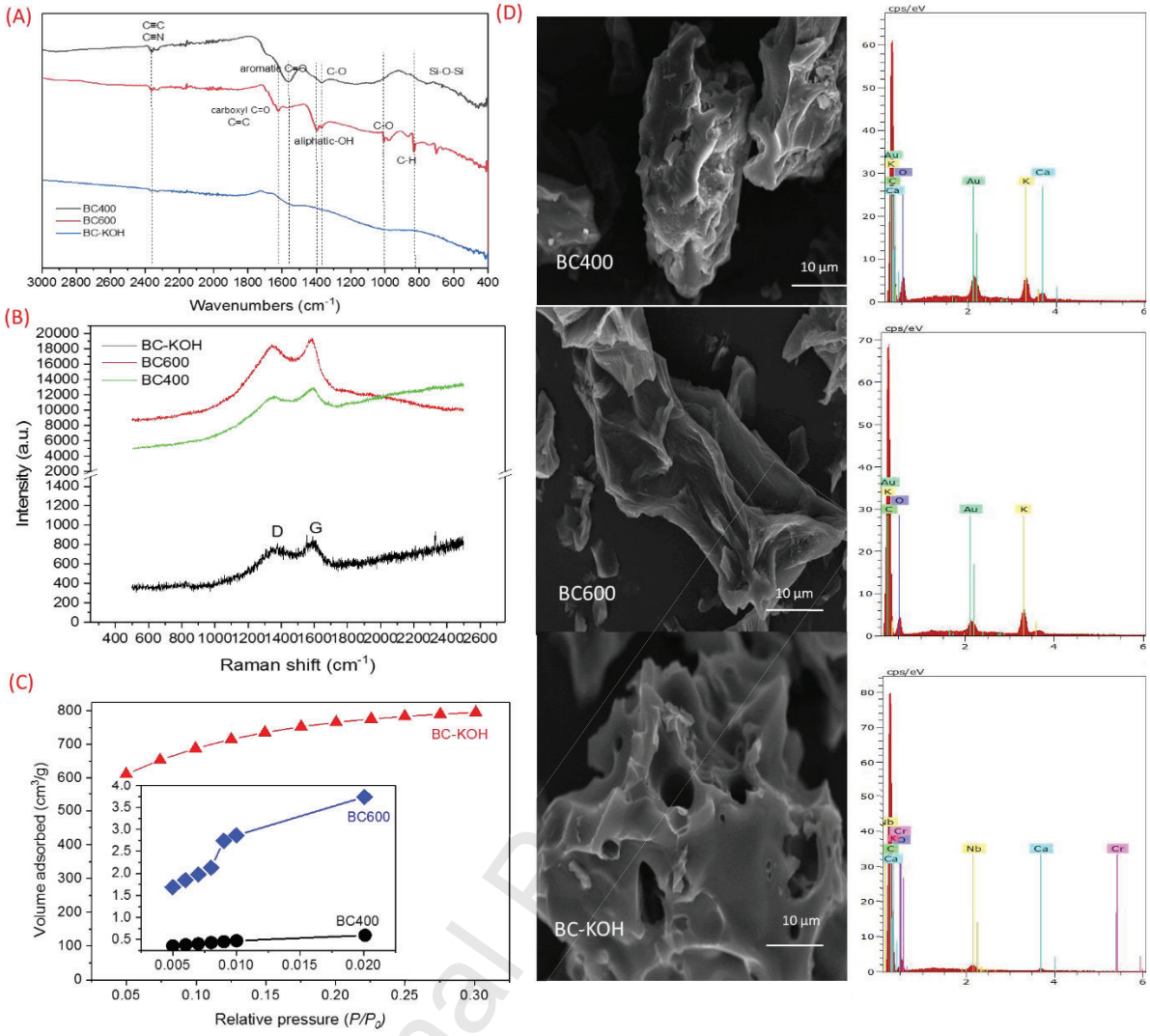

Fig. 1 Characteristics of biochar produced at 400 ℃ (BC-400), 600 ℃ (BC-600) and activated by KOH (BC-KOH): (A) FTIR spectrum; (B) Raman spectrum; (C) BET surface area isotherm; (D) SEM-EDS spectrum.

Raman spectrum of the BC-400, BC-600 and BC-KOH are depicted in Fig. 1 (B). The Raman spectrum of the biochars consists of two prominent peaks at 1350 cm^{-1} (D) and 1590 cm^{-1} (G), which represented the graphitic lattice vibration mode and disorder in the graphitic structure of the biochar (Zhu et al., 2014). Specifically, peak D refers to disordered sp^2-hybridized carbon atoms with vacancies and impurities, while peak G causes from the stretching of sp^2 atomic pairs in the carbon atom ring or carbon chain. It can be assumed that

the carbon atom is bonded to a sp^2 hybridized covalent bond, while electrons which are not involved in hybridization form a π bond (Fan et al., 2016).

The BET surface area and total pore size volume of the produced biochar are shown in Table 1 and Fig. 1(C). An increase in the BET surface area and total pore volume were observed by increasing the pyrolysis temperature from 400 to 600 ℃. A similar result has been reported in other recent studies (Zhao et al., 2018; Zhao et al., 2017). They explained that the increase in the surface area and pore volumes might be caused by the quick release of H_2 and CH_4 and the reaction of aromatic condensation when the temperature rose from 400 to 600 ℃. As well, when the temperature increased, the formation of more pores and a larger surface area was due to the release of more volatiles from the biomass surface (Cheng & Li, 2018). When the BC-400 was further activated by KOH, a huge increase in the surface area (2457.367 m^2/g) and total pore volumes (1.14 cm^3/g) was obtained. This finding was consistent with the observation of the SEM analysis.

The microstructure of BC-400, BC-600 and BC-KOH studied by SEM is displayed in Fig. 1 (D). It can be observed that the BC-400 and BC-600 have a relatively smooth and dense surface. A clear pore structure can be seen on the surface of the BC-KOH, indicating an enhancement in exposed surface area and pore size. As mentioned earlier, the interaction between alkali compounds and carbon promotes the formation of a large surface area (Otawa et al., 1990). For instance, Zhang et al. (2015) produced a highly porous activated carbon from petroleum coke via the KOH activation process at 800 ℃, with a large surface area (2800–2900 m^2/g) and total pore volume (1.4–2.1 cm^3/g). Similarly, Yang et al. (2019a) employed KOH to activate willow branch-derived biochar at 850 ℃ and achieved a large surface area (3342 m^2/g) and total pore volume (1.912 cm^3/g). The increase in the surface area and pore size of biochar by KOH activation is a synergistic effect of several factors (Cheng & Li, 2018). The chemical reaction for the process of KOH activation is shown in Eq. (10-13):

$$6KOH + 2C \rightarrow 2K + 3H_2 \uparrow + 2K_2CO_3 \quad (10)$$

$$6KOH + CO_2 \rightarrow K_2CO_3 + H_2O \uparrow \quad (11)$$

$$K_2CO_3 + 2C \rightarrow K_2O + 2CO \uparrow \quad (12)$$

$$K_2O + CO \rightarrow 2K + CO \uparrow \quad (13)$$

Through the above chemical reactions, the biochar can be activated through the etching process by KOH and its intermediates K_2CO_3 and K_2O. The H_2 and CO produced from chemical reactions can promote the formation of microporosity and macropores on the biochar (Yang et al., 2019a). Furthermore, the produced alkali metal can insert into the biochar matrix to extend the biochar lattice and then enlarge the existing pores (Cheng & Li, 2018).

3.2 Adsorption capacities

By using initial TCs concentration of 10 mg/L, the biochar adsorption capacity over time is shown in Fig. 2. It should be noted that the BC-400 revealed the lowest adsorption of TCs (8.94 mg/g for TC, 11.49 for OTC and 23.80 for CTC), followed by the adsorption capacity of TCs on BC-600 (14.42 mg/g for TC, 16.77 mg/g for OTC and 25.85 mg/g for CTC). Enhancement in adsorption capacity of TC and OTC on corn straw and pineapple peel biochar was also documented by previous researchers when the biochar was obtained at higher temperatures (Fu et al., 2016; Zhang et al., 2012). Under the same adsorption conditions, the adsorption amount of TCs onto BC-KOH sharply increased, with 124.95, 124.91 and 124.99 mg/g for TC, OTC and CTC, respectively. Therefore, a positive correlation was found between the adsorption capacity and surface area/total pore volume of the biochar. Ahmad et al. (2013) indicated that the enhanced porous structure of the biochar surfaces increased the adsorption of organic compounds via a pore-filling mechanism. Additionally, high surface area and pore volume can potentially facilitate faster mass transfer of TCs into the biochar pores and provide more opportunities for the interaction between TCs molecules and the active site (Trakal et al., 2014).

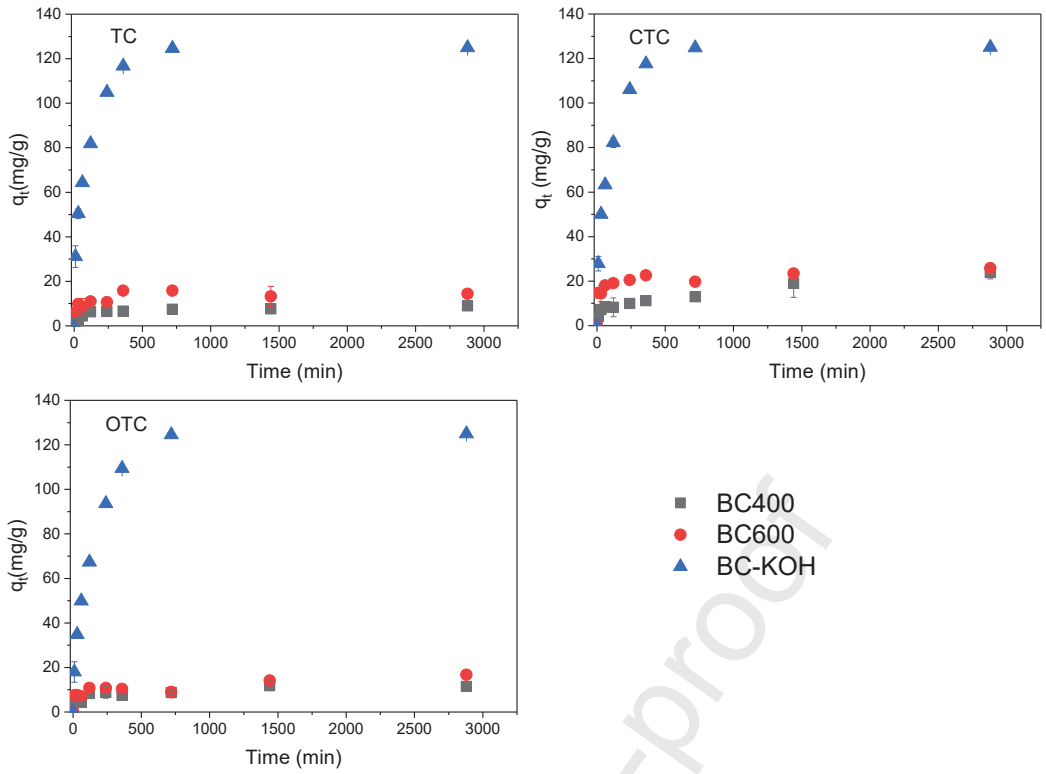

Fig. 2 Adsorption capacity of tetracycline (TC), oxytetracycline (OTC) and chlortetracycline (CTC) on BC-400, BC-600 and BC-KOH (pH=7.0 ±0.5, T=295.15 K).

The decrease in the oxygen content may also have positive effects on the adsorption capacity due to the increased hydrophobic nature of the biochar surface (Taheran et al., 2016). hydrophobic organic compounds are easily adsorbed on biochar with a highly hydrophobic surface (Rivera-Utrilla et al., 2013). Moreover, Rivera-Utrilla et al. (2013) observed that carbons with a low oxygen content had high levels of electron-rich sites in their graphene planes and low concentrations of surface electron-attracting oxygen groups, thereby, enhancing the adsorption of aromatic compounds. The disappearance of peaks at 1560 cm^{-1} in the FTIR spectrum of BC-KOH verified the complete outgassing of hydrophobic groups from BC-400, modifying the affinity of activated biochar for TCs (Gu & Wang, 2013). Overall, BC-KOH emerged as the best biochar for adsorbing TCs and subsequently chosen for further research.

3.3 Adsorption kinetics

Adsorption kinetics study serves to identify the adsorption mechanism and rate-limiting step. Fig. 3 displays the adsorption of TCs onto BC-KOH by using two different initial concentration of TCs (10 and 40 mg/L). From Fig. 3, it is observed that the adsorption could reach equilibrium at approximately 48h after initial contact time, hence, the solutions were shaken for a total period of 75 h in this experiment. As the reaction time increased, the adsorption amount of the two initial concentrations of TCs indicates a similar trend, which increased rapidly at the early stage of the adsorption and then slowed down due to the limited number of active adsorption sites (Peng et al., 2014). As observed from Fig. 3, higher adsorption capacity could be achieved by higher initial concentrations of TCs, ranging from 10 mg/L to 40 mg/L. The possible reason is that higher driving force could be provided by the higher initial concentration to overcome the resistance to TC mass transfer between water and surface of porous carbon (Yang et al., 2019a).

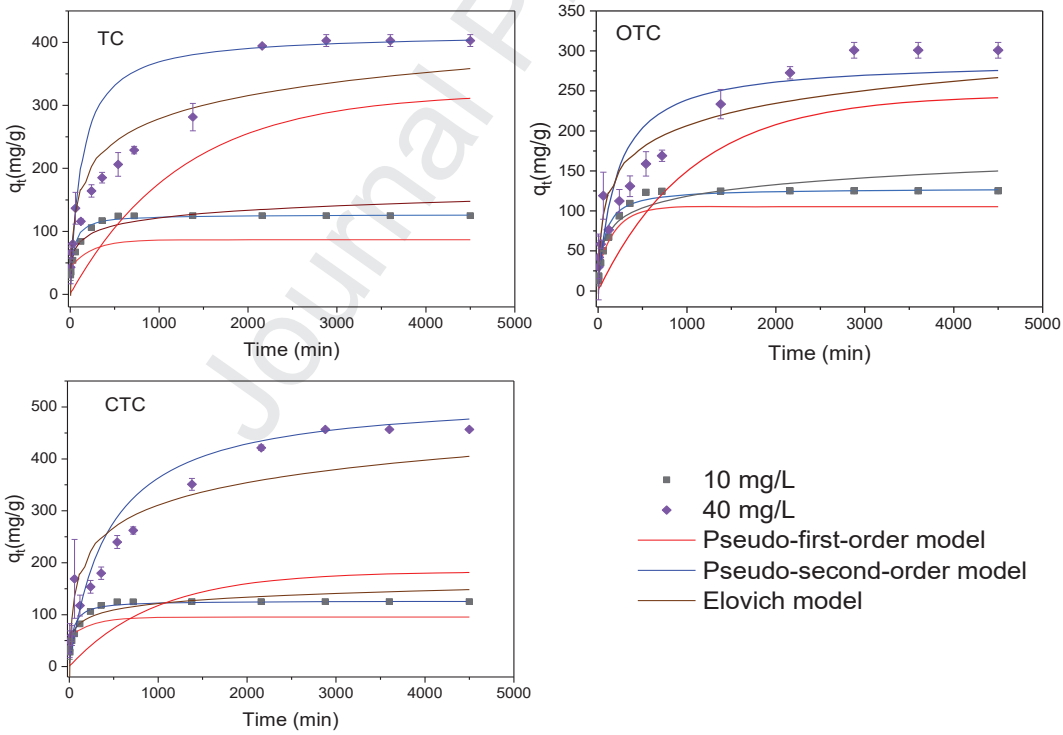

Fig. 3 Adsorption kinetic of tetracycline antibiotics on BC-KOH fitted by pseudo-first-order (PFO), pseudo-second-order (PSO) and Elovich models under two different initial concentrations of TCs.

The PFO, PSO and Evolich kinetic models were widely used to describe the adsorption data, which were presented in Fig. 3. The kinetic parameters of TCs adsorption on BC-KOH are summarized in Table 2. By comparing the correlation coefficient (R^2), the PSO model (R^2: 0.91-1.0) was more appropriate than PFO (R2: 0.88-0.99) and Elovich (R^2: 0.85-0.94) model to fit the adsorption of TC, OTC and CTC to BC-KOH. Furthermore, the adsorption capacity calculated qe^c from PSO equation was more consistent with the experimental qe^e values. This outcome demonstrated that the adsorption rate was consistent with the number of active sites on the surface of BC-KOH and the rate-limiting step was greatly affected by chemisorptive interactions. The finding is consistent with another study's results (Jin et al., 2014). As shown in Table 2, the PSO rate constant (K_2) under low initial concentration (10 mg/L of TCs) was higher than that under high initial concentrations (40 mg/L of TCs), possibly because the competition for available adsorption sites increased at high concentration (He et al., 2016). As well, based on the calculation of the Evolich model, the higher value of a compared to b also reflected the rapid adsorption of TCs at the early stage. Moreover, the high 1/b value suggests the potential of high adsorption capacity of TCs on BC-KOH.

Table 2. Kinetic parameters for the adsorption of tetracycline antibiotics onto BC-KOH

Compound	TC		OTC		CTC	
mg/L	10	40	10	40	10	40
qe^b	124.95	402.86	124.91	300.82	124.99	456.68
Pseudo-first-order						
qe^c	45.2	319.99	78.87	244.93	39.33	182.95
K_1	4.2×10^{-3}	7.99×10^{-4}	5.0×10^{-3}	9.43×10^{-4}	4.0×10^{-3}	1.03×10^{-3}
R^2	0.88	0.89	0.94	0.98	0.9	0.99
Pseudo-second-order						
qe^c	126.58	414.9378	128.21	288.1844	126.58	523.5602
K_2	2.37×10^{-4}	1.92×10^{-5}	1.16×10^{-4}	1.67×10^{-5}	2.17×10^{-4}	4.32×10^{-6}
R^2	1	0.99	1	0.91	1	0.98
Elovich						
a	18.83	10.16	5.83	7.25	15.92	9.09
b	0.059	0.019	0.048	0.025	0.056	0.016
1/b	17.38	53.018	21.033	39.73	17.85	62.43

R^2	0.94	0.86	0.94	0.86	0.92	0.85
Liquid film diffusion						
K_{fd}	4.2×10^{-3}	1.7×10^{-3}	5.0×10^{-3}	1×10^{-3}	4×10^{-3}	1.1×10^{-3}
R^2	0.88	0.84	0.95	0.98	0.8	0.98
Intra-particle diffusion						
K_i	0.21	7.45	0.12	4.68	7.74×10^{-4}	4.77
K_1	4.34	7.62	5.03	5.33	3.25	7.62
K_2	0.2	0.53	3.5×10^{-3}	-2.7×10^{-5}	7.04×10^{-4}	-2.7×10^{-3}
C_i	113.66	41.35	117.82	30.36	124.91	166.02
R_1^2	0.99	1	0.98	0.99	0.88	1

Referring to the porous structure of BC-KOH, the intraparticle diffusion (IPD) and the liquid film diffusion (LFD) model were further used to identify the diffusion mechanism of TCs on BC-KOH. According to previous reports, if the plot of q_t versus $t^{1/2}$ gives a straight line through the origin, intra-particle diffusion is taken to be the only rate-controlling step (Weber & Morris, 1963). As shown in Fig. 4 (d), the q_t versus $t^{1/2}$ gives a straight line ($R1^2$: 0.88-1.0) before reaching adsorption equilibrium, but the line did not cross the origin, which demonstrated that the intra-particle diffusion was dominant in the adsorption process but not the only rate-controlling step (Fierro et al., 2008). Moreover, the R^2 value (0.80-0.98) of the liquid film diffusion model also reflected the fact that the film diffusion partly contributed to the whole adsorption process. Therefore, before reaching the adsorption equilibrium, TCs were transported from the solution to the external surface of BC-KOH by the molecule diffusion and film diffusion only in the early stages of adsorption. Then they entered the internal pore structure and were adsorbed by the interior surface of BC-KOH under the control of intra-particle diffusion. Similar results were reported in other studies which examined the adsorption of TC or other organic matter on porous carbon (Fierro et al., 2008; Jang & Kan, 2019; Zhang et al., 2019). In this study, the positive value of intercepts (C_i) from IPD model also indicated the rapid adsorption of TCs on BC-KOH (Jang & Kan, 2019).

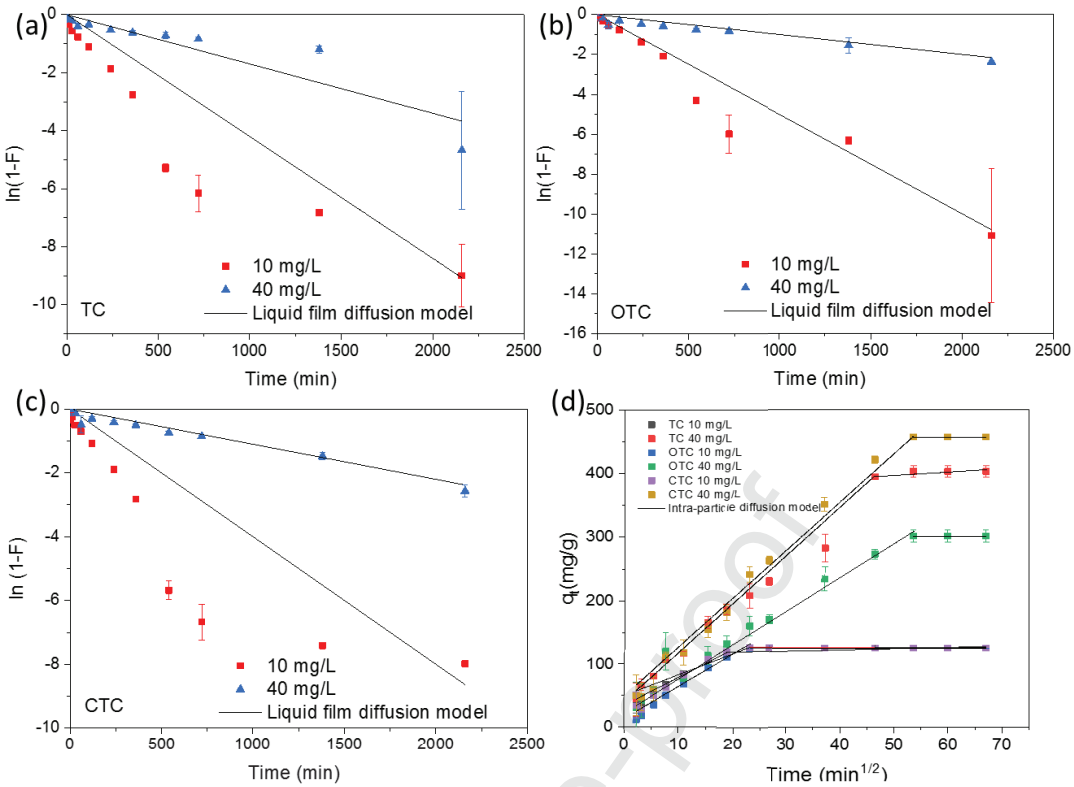

Fig. 4 Adsorption kinetics of tetracycline antibiotics on BC-KOH fitted by the liquid film diffusion (LFD) (a-c) and intraparticle diffusion (IPD) (d) model under two different initial concentrations.

3.4 Adsorption isotherms and effect of temperature

Changes in adsorption isotherm curves can help to analyse the interaction between adsorbate and adsorbent, as well as the adsorption layer characteristics (Jang et al., 2018). The Langmuir and Freundlich models were used to fit the adsorption data of TCs on BC-KOH at 295.5, 303.5 and 313.5 K, respectively, as presented in Fig. 5. The adsorption parameters of these two models are listed in Table 3. Similarly, an increasing trend in the adsorption capacity of BC-KOH was found by increasing the initial concentration of TCs. In the whole concentration range, it was observed that the adsorption capacity of TCs rose by increasing temperature, indicating that the adsorption process is an endothermic one and operates favorably under higher temperature.

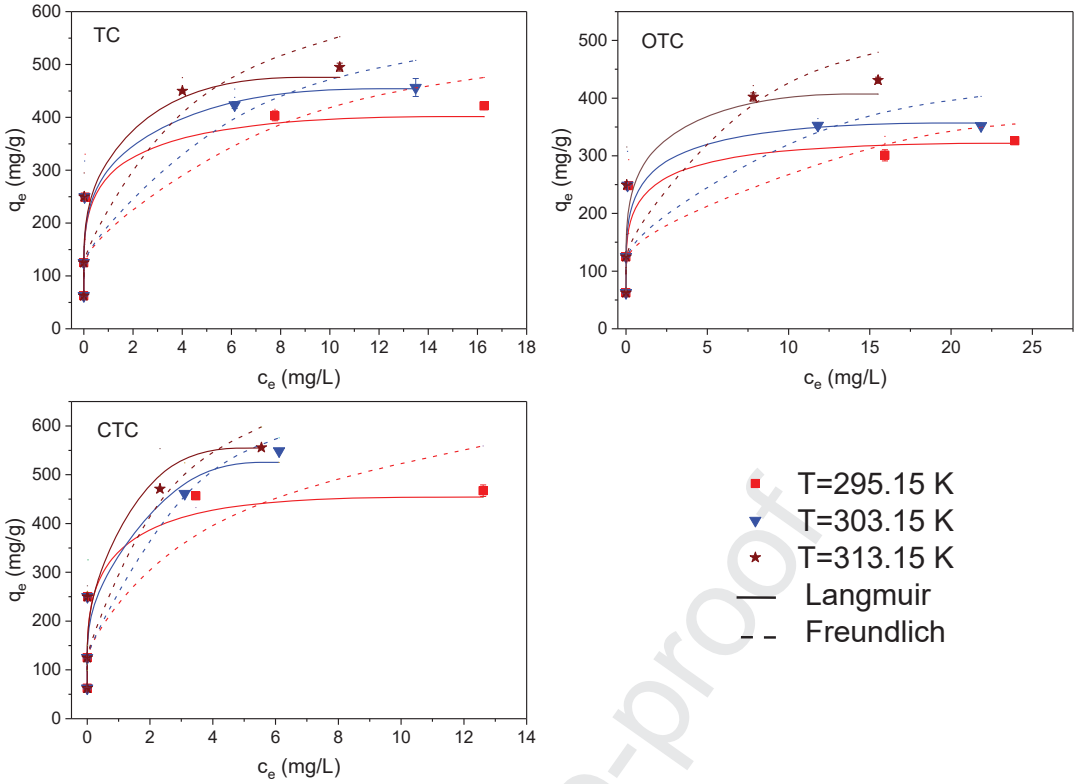

Fig. 5 Adsorption isotherms of tetracycline antibiotics adsorbed onto BC-KOH fitted by Langmuir and Freundlich models at different temperatures.

Table 3. Langmuir and Freundlich isotherm parameters of the adsorption of tetracycline antibiotics on BC-KOH

	TC			OTC			CTC		
T (K)	295.15	303.15	313.15	295.15	303.15	313.15	295.15	303.15	313.15
	Langmuir model								
q_m	401.61	454.55	476.19	322	357.14	407.5	454.55	526	555.56
K_L	80.32	80.44	116.74	62.37	68.81	66.72	93.68	118.7	127.46
R_L	0.00025-0.0025	0.00025-0.0025	0.00019-0.0017	0.00033-0.0033	0.00029-0.0029	0.0003-0.003	0.00021-0.0021	0.00016-0.0016	0.00016-0.0016
R^2	0.94	0.94	0.97	0.96	0.96	0.97	0.96	0.99	0.99
	Freundlich model								
K_f	285.15	311.59	352.59	218.09	243.25	286.55	338.29	397.62	418.05
1/n	0.18	0.19	0.19	0.15	0.16	0.19	0.20	0.20	0.21
R^2	0.86	0.84	0.85	0.8	0.82	0.85	0.86	0.85	0.85

It was observed that the Langmuir model could fit the experimental data better than the Freundlich model, with higher related coefficients (R^2 = 0.94-0.99). This may be related to the monolayer adsorption of TCs onto the external and internal surfaces of the porous biochar (Yang et al., 2019a). Moreover, the very low R_L values listed in Table 3 indicated the Langmuir isotherm model is favorable (Tang et al., 2018). The values of 1/n from the Freundlich model, which is in the range of 0 to 1, indicated the high affinity between TCs and BC-KOH, suggesting the adsorption was a favorable process (Fan et al., 2016). The maximum adsorption capacities (q_m) of BC-KOH calculated from the Langmuir model under the studied temperatures were 401.61-476.19 mg/g for TC, 322-407.5 mg/g for OTC and 454.55-555.56 mg/g for CTC, respectively. Table 4 compares the maximum adsorption capacity for TCs on various agriculture waste-derived biochar reported in previous studies. It is indicated that the BC-KOH produced from pomelo peel in this research is an excellent adsorbent for removing TC, OTC and CTC from aqueous solution simultaneously.

Table 4. Comparison of maximum adsorption for tetracycline antibiotics on various agriculture waste-derived biochar reported in previous studies

Adsorbents	Surface area (m^2/g)	Total pore volume (cm^3/g)	Adsorbate	q_m (mg/g)	References
Rice straw biochar	372.2	0.23	TC	167.5	(Chen et al., 2018)
Rice straw biochar	27.66	0.059	TC	13.85	(Wang et al., 2017)
Macadamia nut shell biocahr	1524	0.826	TC	455.33	(Martins et al., 2015)
Rice husk biochar	211.76	0.121	TC	80.9	(Zeng et al., 2018)
Waste Auricularia auricula dregs biochar	46.56	0.06	TC	11.9	(Dai et al., 2020)
Cassava waste biochar	128.42	0.01	OTC	10	(Luo et al., 2018)
Swine manure biochar	319.04	0.25	TC	160.3	(Chen et al., 2018)
Cow manure biochar	31.23	0.0234	TC	22.553	(Zhang et al., 2019)
Waste chicken bones biochar	328.06	0.0028	TC	98.89	(Oladipo & Ifebajo, 2018)

Waste chicken feather biochar	1838	1.033	TC	388.33	(Li et al., 2017)
Pomelo peel biochar	2457.367	1.14	TC OTC CTC	476.19 407.5 555.56	This study

3.5 Influence of initial pH on the adsorption

The solution pH value can affect the adsorption processes considering its effect on surface charges of the biochar and the TCs molecules species. The TCs molecules are almost in a cation form at pH < 3.3, in a zwitterion form in the pH ranging from 3.3 to 7.8 and in an anion form at pH > 7.8 (Yang et al., 2011). With the increase of pH, the TCs become more negative. In this study, the influence of pH on the adsorption of TCs onto BC-KOH was assessed by changing the pH value of initial solution from 1.5 to 10. Fig. 6 shows the adsorption capacity of TCs on BC-KOH (a) and the zeta potential of biochar before and after TCs adsorption (b) at different pH values. The BC-KOH surface was positively charged at pH < 3.2, which becomes negatively charged at pH > 3.2. An increasing trend in adsorption capacity of TCs was found by elevating the pH from 1.5 to 8.5. At the pH < 3.2, the relatively small amount of adsorption was due to the electrostatic repulsions between the cationic species of three antibiotics in solution and the positively charged surface of the BC-KOH. The adsorption capacity increased by raising the pH from 3.2 to 7.8, due to the repulsive force which decreased gradually since TCs mainly exist in zwitterion form. By increasing the pH from 3.2 to 7.8, the zeta potential of the biochar after adsorption was increased through adsorbing the TCs molecular on its surface. Interestingly enough, the maximum adsorption capacity at equilibrium was obtained at pH=8.5, although the negatively charged BC-KOH indicated its repulsion of anionic TCs. Therefore, adsorption of TCs onto the BC-KOH can be affected by the initial solution pH, however, the electrostatic interaction only contributed to a part of the adsorption mechanism. Similar results have been found by the adsorption of TCs from aqueous solutions on a multi-walled carbon nanotube (Xiong et al., 2018). As can be

seen from Fig. 6 (a), the adsorption amount of TCs was still high at the lower and higher pH value (pH<3.2 or >8.5). It is proved that BC-KOH can be applied in swine wastewater treatment broadly considering its good adsorption properties in a wide range of pH (from 1.5 to 10) (Tang et al., 2018).

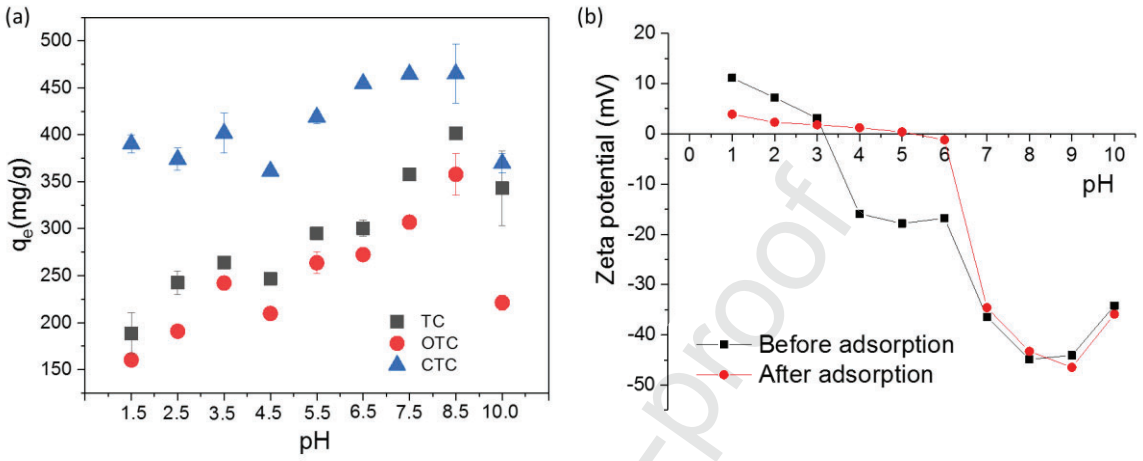

Fig. 6 The adsorption capacity of tetracycline antibiotics on BC-KOH (a) and the zeta potential of biochar before and after adsorption (b) at different pH values.

3.6 Potential mechanisms of the adsorption

The potential mechanisms regarding the adsorption of TCs on BC-KOH can be suggested through the above analysis of the biochar characteristics, the chemical structure of TCs, the fitted adsorption kinetics and isotherm models, as well as the effects of pH on adsorption. A positive correlation was found between the adsorption capacity of TCs and the surface area/total pore size of the biochar. The large surface area and total pore size of BC-KOH resulting from SEM and BET suggested that pore filling was a major adsorption mechanism. The adsorption kinetics data of TCs on BC-KOH indicated that pore filling and chemisorption were the main for the adsorption of TCs from wastewater (Premarathna et al., 2019). The fit of the data with the Langmuir model also suggested the monolayer adsorption process.

According to the Raman analysis results, graphitic layers did exist in the structure of the biochar, which can function as a π-π acceptor (Jin et al., 2014). Hence, the adsorption of TCs on BC-KOH can occur between the π-electrons in the graphene layers of the biochar and the π-electrons in the aromatic rings of TCs through the π-π electron donor–acceptor (π-π EDA) mechanism (Gao et al., 2012; Ji et al., 2009; Rivera-Utrilla et al., 2013). This is consistent with the study by Liu et al. (2012), who demonstrated that the alkali-activated biochar facilitates the formation of π – π interactions between the ring structure of TC molecules and the biochar's graphite-like sheets. Liu et al. (2012) asserted that the graphite-like structure of biochar promoted the π–π interactions between the biochar and the aromatic rings of CTC. Furthermore, based on the above discussion, the adsorption of TCs on BC-KOH can be affected by the initial solution pH, suggesting the potential mechanism of electrostatic interaction. Conversely, the relatively large amount of TCs adsorbed at a pH value up to 8.5 may result from the adsorption mechanisms of pore filling and π-π adsorbate-adsorbent interactions.

3.7 TCs removal from synthetic swine wastewater

The removal efficiency of TCs by the adsorption of BC-KOH from deionized water and synthetic swine wastewater was showed displayed in Fig. 7. As can be seen in Fig. 7, almost 100% of TCs could be removal from deionized water in 75 h with the initial concentration of 10 mg/L, whereas, the average removal efficiency of TC, OTC and CTC decreased to 85. 04%, 82.17% and 96.64%, respectively, in the synthetic swine wastewater. The reduced adsorption of trace elements onto biochar in wastewater compared to the removal in deionized water was also observed by a previous report (Ahmed et al., 2018). Such result indicated that the presence of other compounds in the wastewater inhibited the adsorption of TCs onto BC-KOH. The inhibition could be caused by the competitive adsorption between TCs and other pollutants for the specific sites and pore filling on BC-KOH (Premarathna et al., 2019). Nevertheless, there were still more than 80% of TCs could be removed from wastewater

through the adsorption of BC-KOH. Considering the relatively low concentration of TCs in the real swine wastewater, BC-KOH can be used as an effective adsorbent to remove TCs from swine wastewater even under the influence of other pollutants.

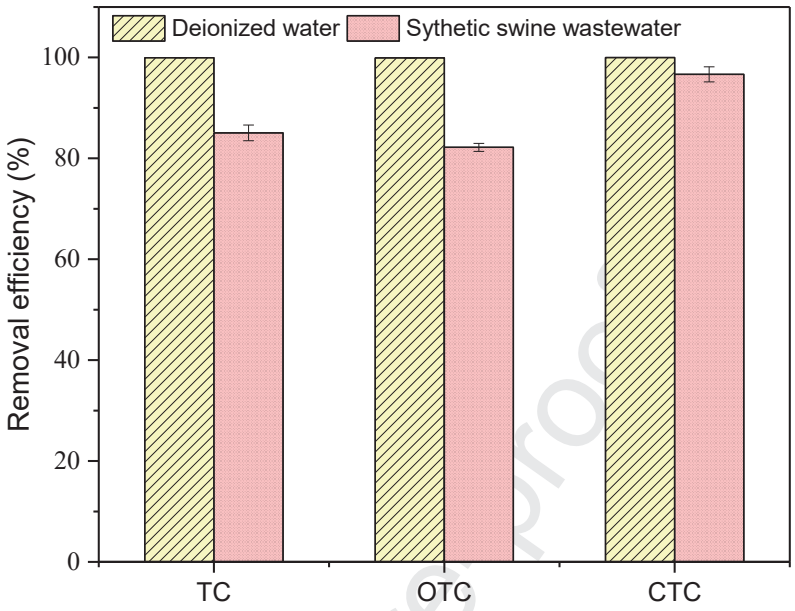

Fig. 7 Removal efficiency of TCs (10 mg/L) by the adsorption of BC-KOH from deionized water and synthetic swine wastewater in 75 h at pH 7.0 ±0.5 and 294.15 K.

3.8 Economic feasibility

To assess the large-scale application of biochar on the adsorption removal of antibiotics from swine wastewater, the economic performance of biochar compared with activated carbon was considered in this study. The production cost of biochar mainly relates to the cost of feedstock materials, production cost and other additional cost, which can be estimated and calculated by Eq. (14):

$$\text{Total biochar production cost} = \text{feedstock cost} + \text{production cost} + \text{additional other cost} \quad (14)$$

Based on this study, the total cost of producing 1 kg pomelo peel derived biochar (BC-KOH) was estimated as follows:

The feedstock cost is USD $ 5.69 (including pomelo peels collection cost and KOH cost). The production cost is USD$ 2.42 (including the cost of electricity consumption for drying and carbonization). The cost for others such as washing, grinding and transporting is USD $ 1.71. Therefore, the total cost for generating per kg BC-KOH was USD $ 9.82, which is cheaper than commercial activated carbon (up to USD $45.71/kg) as sold in Henan Huasheng Charcoal Industry Ltd. (http://hnhsty.com/).

Commercial activated carbons are commonly produced from expensive and non-renewable materials, such as natural coal, wood, peat and petroleum residues, by pyrolysis and the following physical activation at high temperatures (700-1100 ℃) (Allen et al., 1998). From this point of view, using pomelo peel wastes as the raw material to produce biochar in this study not only save the cost of raw materials but also save the cost of waste disposal. From the perspective of energy saving, chemical activation is commonly chosen for activating the carbon material due to the lower temperature and shorter time requirement than that of physical activation (Mohammad et al., 2009). The common method of chemical activation was using chemicals such as H_3PO_4, KOH, or NaOH followed by heating under a gas (nitrogen) flow at the temperature between 450 and 900◦C (Gupta et al., 2009). Thus, less energy would be consumed for the production of the biochar in this study at lower temperature.

The adsorption capacity of carbon for antibiotics is also an important factor for cost analysis. For commercial activated carbons, the surface areas generally vary in the range between 500 and 2000 m^2/g (Gupta et al., 2009), while a relative large surface area was observed for the biochar produced in this study (2457.37 m^2/g). As reviewed by Ahmed et al. (2017b), the dosage used for the adsorption of individual tetracycline antibiotics onto activated carbon was mainly in the range of 0.2 g/L to 20 g/L. In comparison, the dosage of BC-KOH used in the present study was 0.08 g/L with comparable adsorption capacity for adsorbing TC, OTC and CTC simultaneously. Therefore, compared to the commercial

activated carbon, the BC-KOH has high potential for large-scale application.

4. Conclusion

The developed new pomelo peel derived biochar in this study was proved to be a promising adsorbent for removing tetracycline antibiotics from swine wastewater in a cost-effective and environmentally friendly manner. The experimental results indicated that large BET surface area and total pore volume biochar (BC-KOH) could be obtained by further activating of BC-400 by KOH at 600 ℃. The adsorption capacity of TCs was positive with the surface area and pore volume of the biochar. The adsorption data fitted well by the pseudo-second-order kinetic model and Langmuir isotherm model. Mechanisms of pore filling, electrostatic interaction and π–π interactions between the adsorbent and adsorbate may constitute the main adsorption of TCs onto BC-KOH.

Acknowledgement

This research was supported by the Centre for Technology in Water and Wastewater, University of Technology Sydney, Australia (UTS, RIA NGO) and the Korea Institute of Energy Technology Evaluation and Planning (KETEP) and the Ministry of Trade, Industry & Energy (MOTIE) of the Republic of Korea (Grant No. 20173010092470).

References

1. Ahmad, M., Lee, S.S., Rajapaksha, A.U., Vithanage, M., Zhang, M., Cho, J.S., Lee, S.-E., Ok, Y.S., 2013. Trichloroethylene adsorption by pine needle biochars produced at various pyrolysis temperatures. Bioresour. Technol., **143**, 615-622.

2. Ahmad, M., Rajapaksha, A.U., Lim, J.E., Zhang, M., Bolan, N., Mohan, D., Vithanage, M., Lee, S.S., Ok, Y.S., 2014. Biochar as a sorbent for contaminant management in soil and water: a review. Chemosphere, **99**, 19-33.

3. Ahmed, M.B., Zhou, J.L., Ngo, H.H., Guo, W., 2015. Adsorptive removal of antibiotics from water and wastewater: progress and challenges. Sci. Total Environ., **532**, 112-126.

4. Ahmed, M.B., Zhou, J.L., Ngo, H.H., Guo, W., Johir, M.A.H., Belhaj, D., 2017a. Competitive sorption affinity of sulfonamides and chloramphenicol antibiotics toward functionalized biochar for water and wastewater treatment. Bioresour. Technol., **238**, 306-312.

5. Ahmed, M.B., Zhou, J.L., Ngo, H.H., Johir, M.A.H. and Sornalingam, K., 2018. Sorptive removal of phenolic endocrine disruptors by functionalized biochar: Competitive interaction mechanism, removal efficacy and application in wastewater. Chem. Eng. J., **335**, 801-811.

6. Ahmed, M.J., 2017b. Adsorption of quinolone, tetracycline, and penicillin antibiotics from aqueous solution using activated carbons. Environ. Toxicol. Pharmacol., **50**, 1-10.

7. Allen, S.J., Whitten, L. and McKay, G., 1998. The production and characterisation of activated carbons: a review. Dev. Chem. Eng. Min. Process., **6** (5), 231-261.

8. Ben, W., Qiang, Z., Pan, X., Nie, Y., 2011. Degradation of veterinary antibiotics by ozone in swine wastewater pretreated with sequencing batch reactor. J. Environ. Eng., **138** (3), 272-277.

9. Chen, T., Luo, L., Deng, S., Shi, G., Zhang, S., Zhang, Y., Deng, O., Wang, L., Zhang, J., Wei, L., 2018. Sorption of tetracycline on H3PO4 modified biochar derived from rice straw and swine manure. Bioresour. Technol., **267**, 431-437.

10. Chen, Y., Shi, J., Du, Q., Zhang, H., Cui, Y., 2019. Antibiotic removal by agricultural waste biochars with different forms of iron oxide. RSC Advances, **9** (25), 14143-14153.

11. Cheng, D., Ngo, H., Guo, W., Chang, S., Nguyen, D., Kumar, S.M., Du, B., Wei, Q., Wei, D., 2018a. Problematic effects of antibiotics on anaerobic treatment of swine wastewater. Bioresour. Technol., **263**, 642-653.

12. Cheng, D., Ngo, H., Guo, W., Liu, Y., Zhou, J., Chang, S., Nguyen, D., Bui, X., Zhang, X., 2018b. Bioprocessing for elimination antibiotics and hormones from swine wastewater. Sci. Total Environ., **621**, 1664-1682.

13. Cheng, D., Ngo, H.H., Guo, W., Chang, S.W., Nguyen, D.D., Liu, Y., Wei, Q., Wei, D., 2019. A critical review on antibiotics and hormones in swine wastewater: Water pollution problems and control approaches. J. Hazard. Mater., 121682.

14. Cheng, F., Li, X., 2018. Preparation and application of biochar-based catalysts for biofuel production. Catalysts, **8** (9), 346.

15. Dai, Y., Li, J., Shan, D., 2020. Adsorption of tetracycline in aqueous solution by biochar derived from waste Auricularia auricula dregs. Chemosphere, **238**, 124432.

16. Dai, Y., Zhang, N., Xing, C., Cui, Q., Sun, Q., 2019. The adsorption, regeneration and engineering applications of biochar for removal organic pollutants: A review. Chemosphere.

17. Enders, A., Hanley, K., Whitman, T., Joseph, S., Lehmann, J., 2012. Characterization of biochars to evaluate recalcitrance and agronomic performance. Bioresour. Technol., **114**, 644-653.

18. Fan, H.-T., Shi, L.-Q., Shen, H., Chen, X., Xie, K.-P., 2016. Equilibrium, isotherm, kinetic and thermodynamic studies for removal of tetracycline antibiotics by adsorption onto hazelnut shell derived activated carbons from aqueous media. RSC Advances, **6** (111), 109983-109991.

19. Fierro, V., Torné-Fernández, V., Montané, D., Celzard, A., 2008. Adsorption of phenol onto activated carbons having different textural and surface properties. Microporous Mesoporous Mater., **111** (1-3), 276-284.

20. Fu, B., Ge, C., Yue, L., Luo, J., Feng, D., Deng, H., Yu, H., 2016. Characterization of biochar derived from pineapple peel waste and its application for sorption of oxytetracycline from aqueous solution. BioResources, **11** (4), 9017-9035.

21. Gao, Y., Li, Y., Zhang, L., Huang, H., Hu, J., Shah, S.M., Su, X., 2012. Adsorption and removal of tetracycline antibiotics from aqueous solution by graphene oxide. J. Colloid Interface Sci., **368** (1), 540-546.

22. Gu, Z., Wang, X., 2013. Carbon materials from high ash bio-char: a nanostructure similar to activated graphene. Am. Trans. Eng. Appl. Sci, **2** (1), 15-34.

23. Gupta, V.K., Carrott, P.J.M., Ribeiro Carrott, M.M.L. and Suhas, 2009. Low-cost adsorbents: growing approach to wastewater treatment—a review. Crit. Rev. Environ. Sci. Technol., **39** (10), 783-842.

24. He, J., Dai, J., Zhang, T., Sun, J., Xie, A., Tian, S., Yan, Y., Huo, P., 2016. Preparation of highly porous carbon from sustainable α-cellulose for superior removal performance of tetracycline and sulfamethazine from water. RSC Advances, **6** (33), 28023-28033.

25. Jang, H.M., Kan, E., 2019. A novel hay-derived biochar for removal of tetracyclines in water. Bioresour. Technol., **274**, 162-172.

26. Jang, H.M., Yoo, S., Choi, Y.-K., Park, S., Kan, E., 2018. Adsorption isotherm, kinetic modeling and mechanism of tetracycline on Pinus taeda-derived activated biochar. Bioresour. Technol., **259**, 24-31.

27. Ji, L., Chen, W., Duan, L., Zhu, D., 2009. Mechanisms for strong adsorption of tetracycline to carbon nanotubes: a comparative study using activated carbon and graphite as adsorbents. Environ. Sci. Technol., **43** (7), 2322-2327.

28. Jin, H., Capareda, S., Chang, Z., Gao, J., Xu, Y., Zhang, J., 2014. Biochar pyrolytically produced from municipal solid wastes for aqueous As (V) removal: adsorption property and its improvement with KOH activation. Bioresour. Technol., **169**, 622-629.

29. Kim, D.P., Saegerman, C., Douny, C., Dinh, T.V., Xuan, B.H., Vu, B.D., Hong, N.P., Scippo, M.-L., 2013. First survey on the use of antibiotics in pig and poultry production in the Red River Delta region of Vietnam. Food Public Health, **3** (5), 247-56.

30. Komnitsas, K.A., Zaharaki, D., 2016. Morphology of modified biochar and its potential for phenol removal from aqueous solutions. Frontiers in Environmental Science, **4**, 26.

31. Li, H., Hu, J., Meng, Y., Su, J., Wang, X., 2017. An investigation into the rapid removal of tetracycline using multilayered graphene-phase biochar derived from waste chicken feather. Sci. Total Environ., **603**, 39-48.

32. Liang, Q., Ye, L., Huang, Z.-H., Xu, Q., Bai, Y., Kang, F., Yang, Q.-H., 2014. A honeycomb-like porous carbon derived from pomelo peel for use in high-performance supercapacitors. Nanoscale, **6** (22), 13831-13837.

33. Liu, L., Liu, C., Zheng, J., Huang, X., Wang, Z., Liu, Y., Zhu, G., 2013. Elimination of veterinary antibiotics and antibiotic resistance genes from swine wastewater in the vertical flow constructed wetlands. Chemosphere, **91** (8), 1088-1093.

34. Liu, P., Liu, W.-J., Jiang, H., Chen, J.-J., Li, W.-W., Yu, H.-Q., 2012. Modification of bio-char derived from fast pyrolysis of biomass and its application in removal of tetracycline from aqueous solution. Bioresour. Technol., **121**, 235-240.

35. Luo, J., Li, X., Ge, C., Müller, K., Yu, H., Huang, P., Li, J., Tsang, D.C., Bolan, N.S., Rinklebe, J., 2018. Sorption of norfloxacin, sulfamerazine and oxytetracycline by KOH-modified biochar under single and ternary systems. Bioresour. Technol., **263**, 385-392.

36. Martínez, J.L., 2008. Antibiotics and antibiotic resistance genes in natural environments. Sci, **321** (5887), 365-367.

37. Martins, A.C., Pezoti, O., Cazetta, A.L., Bedin, K.C., Yamazaki, D.A., Bandoch, G.F., Asefa, T., Visentainer, J.V., Almeida, V.C., 2015. Removal of tetracycline by NaOH-activated carbon produced from macadamia nut shells: kinetic and equilibrium studies. Chem. Eng. J., **260**, 291-299.

38. Miyata, M., Ihara, I., Yoshid, G., Toyod, K., Umetsu, K., 2011. Electrochemical oxidation of tetracycline antibiotics using a Ti/IrO2 anode for wastewater treatment of animal husbandry. Water Sci. Technol., **63** (3), 456-461.

39. Mohammad-Khah, A. and Ansari, R., 2009. Activated charcoal: preparation, characterization and applications: a review article. Int. J. Chem. Tech. Res., **1** (4), 859-864.

40. Oladipo, A.A., Ifebajo, A.O., 2018. Highly efficient magnetic chicken bone biochar for removal of tetracycline and fluorescent dye from wastewater: two-stage adsorber analysis. J. Environ. Manage., **209**, 9-16.

41. Otawa, T., Yamada, M., Tanibata, R., Kawakami, M. 1990. Preparation, pore analysis and adsorption behavior of high surface area active carbon from coconut shell. *Proceeding of the international symposium on gas separation technology. Antwerp (Belgium): Elsevier*. pp. 263-70.

42. Peng, B., Chen, L., Que, C., Yang, K., Deng, F., Deng, X., Shi, G., Xu, G., Wu, M., 2016. Adsorption of antibiotics on graphene and biochar in aqueous solutions induced by π-π interactions. Sci. Rep., **6**, 31920.

43. Peng, L., Ren, Y., Gu, J., Qin, P., Zeng, Q., Shao, J., Lei, M., Chai, L., 2014. Iron improving bio-char derived from microalgae on removal of tetracycline from aqueous system. Environmental Science and Pollution Research, **21** (12), 7631-7640.

44. Premarathna, K., Rajapaksha, A.U., Sarkar, B., Kwon, E.E., Bhatnagar, A., Ok, Y.S., Vithanage, M., 2019. Biochar-based engineered composites for sorptive decontamination of water: A review. Chem. Eng. J., **372**, 536-550.

45. Qiang, Z., Macauley, J.J., Mormile, M.R., Surampalli, R., Adams, C.D., 2006. Treatment of antibiotics and antibiotic resistant bacteria in swine wastewater with free chlorine. J. Agric. Food Chem., **54** (21), 8144-8154.

46. Rivera-Utrilla, J., Gómez-Pacheco, C.V., Sánchez-Polo, M., López-Peñalver, J.J., Ocampo-Pérez, R., 2013. Tetracycline removal from water by adsorption/bioadsorption on activated carbons and sludge-derived adsorbents. J. Environ. Manage., **131**, 16-24.

47. Romero-Cano, L.A., González-Gutiérrez, L.V., Baldenegro-Pérez, L.A., Carrasco-Marín, F., 2017. Grapefruit peels as biosorbent: characterization and use in batch and fixed bed column for Cu (II) uptake from wastewater. J. Chem. Technol. Biotechnol., **92** (7), 1650-1658.

48. Song, X.Y., Pan, G.X., Bai, Y.W., Liang, F., Xing, J.J., Gao, J. and Shi, F.N., 2019. Preparation and electrochemical properties of biochar from pyrolysis of pomelo peel via different methods. Fuller. Nanotub. Car. N., **27** (5), 453-458.

49. Sial, T. A., Lan, Z., Khan, M. N., Zhao, Y., Kumbhar, F., Liu, J., Memon, M. 2019. Evaluation of orange peel waste and its biochar on greenhouse gas emissions and soil biochemical properties within a loess soil. Waste Manage., **87**, 125-134.

50. Taheran, M., Naghdi, M., Brar, S.K., Knystautas, E.J., Verma, M., Ramirez, A.A., Surampalli, R.Y., Valéro, J.R., 2016. Adsorption study of environmentally relevant concentrations of chlortetracycline on pinewood biochar. Sci. Total Environ., **571**, 772-777.

51. Tang, L., Yu, J., Pang, Y., Zeng, G., Deng, Y., Wang, J., Ren, X., Ye, S., Peng, B., Feng, H., 2018. Sustainable efficient adsorbent: alkali-acid modified magnetic biochar derived from sewage sludge for aqueous organic contaminant removal. Chem. Eng. J., **336**, 160-169.

52. Trakal, L., Šigut, R., Šillerová, H., Faturíková, D., Komárek, M., 2014. Copper removal from aqueous solution using biochar: effect of chemical activation. Arabian Journal of Chemistry, **7** (1), 43-52.

53. Uchimiya, M., Wartelle, L.H., Klasson, K.T., Fortier, C.A., Lima, I.M., 2011. Influence of pyrolysis temperature on biochar property and function as a heavy metal sorbent in soil. J. Agric. Food Chem., **59** (6), 2501-2510.

54. Wang, H., Chu, Y., Fang, C., Huang, F., Song, Y., Xue, X., 2017. Sorption of tetracycline on biochar derived from rice straw under different temperatures. PLoS ONE, **12** (8), e0182776.

55. Wang, H., Zhang, J., Yuan, X., Jiang, L., Xia, Q., Chen, H., 2019. Photocatalytic removal of antibiotics from natural water matrices and swine wastewater via Cu (I) coordinately polymeric carbon nitride framework. Chem. Eng. J., 123638.

56. Weber, W.J., Morris, J.C., 1963. Kinetics of adsorption on carbon from solution. Journal of the Sanitary Engineering Division, **89** (2), 31-60.

57. Xiong, W., Zeng, G., Yang, Z., Zhou, Y., Zhang, C., Cheng, M., Liu, Y., Hu, L., Wan, J., Zhou, C., 2018. Adsorption of tetracycline antibiotics from aqueous solutions on nanocomposite multi-walled carbon nanotube functionalized MIL-53 (Fe) as new adsorbent. Sci. Total Environ., **627**, 235-244.

58. Yang, J., Dai, J., Wang, L., Ge, W., Xie, A., He, J., Yan, Y., 2019a. Ultrahigh adsorption of tetracycline on willow branche-derived porous carbons with tunable pore structure: Isotherm, kinetics, thermodynamic and new mechanism study. Journal of the Taiwan Institute of Chemical Engineers, **96**, 473-482.

59. Yang, W., Zheng, F., Lu, Y., Xue, X., Li, N., 2011. Adsorption interaction of tetracyclines with porous synthetic resins. Ind. Eng. Chem. Res., **50** (24), 13892-13898.

60. Yang, X., Zhang, S., Ju, M., Liu, L., 2019b. Preparation and modification of biochar materials and their application in soil remediation. Applied Sciences, **9** (7), 1365.

61. Zeng, Z.w., Tian, S.r., Liu, Y.g., Tan, X.f., Zeng, G.m., Jiang, L.h., Yin, Z.h., Liu, N., Liu, S.b., Li, J., 2018. Comparative study of rice husk biochars for aqueous antibiotics removal. J. Chem. Technol. Biotechnol., **93** (4), 1075-1084.

62. Zhang, B., Wu, Y. and Cha, L., 2020. Removal of methyl orange dye using activated biochar derived from pomelo peel wastes: Performance, isotherm, and kinetic studies. J. Disper. Sci. Technol., **41**(1), 125-136.

63. Zhang, D., Yin, J., Zhao, J., Zhu, H., Wang, C., 2015. Adsorption and removal of tetracycline from water by petroleum coke-derived highly porous activated carbon. Journal of Environmental Chemical Engineering, **3** (3), 1504-1512.

64. Zhang, G., Liu, X., Sun, K., He, F., Zhao, Y., Lin, C., 2012. Competitive sorption of metsulfuron-methyl and tetracycline on corn straw biochars. J Environ Qual, **41** (6), 1906-1915.

65. Zhang, M., Li, A., Zhou, Q., Shuang, C., Zhou, W., Wang, M., 2014. Effect of pore size distribution on tetracycline adsorption using magnetic hypercrosslinked resins. Microporous Mesoporous Mater., **184**, 105-111.

66. Zhang, P., Li, Y., Cao, Y., Han, L., 2019. Characteristics of tetracycline adsorption by cow manure biochar prepared at different pyrolysis temperatures. Bioresour. Technol., **285**, 121348.

67. Zhang, W., Sturm, B.S., Knapp, C.W., Graham, D.W., 2009. Accumulation of tetracycline resistance genes in aquatic biofilms due to periodic waste loadings from swine lagoons. Environ. Sci. Technol., **43** (20), 7643-7650.

68. Zhao, B., O'Connor, D., Zhang, J., Peng, T., Shen, Z., Tsang, D.C., Hou, D., 2018. Effect of pyrolysis temperature, heating rate, and residence time on rapeseed stem derived biochar. Journal of cleaner production, **174**, 977-987.

69. Zhao, S.-X., Ta, N., Wang, X.-D., 2017. Effect of temperature on the structural and physicochemical properties of biochar with apple tree branches as feedstock material. Energies, **10** (9), 1293.

70. Zhu, X., Li, C., Li, J., Xie, B., Lü, J., Li, Y., 2018. Thermal treatment of biochar in the air/nitrogen atmosphere for developed mesoporosity and enhanced adsorption to tetracycline. Bioresour. Technol., **263**, 475-482.

71. Zhu, X., Liu, Y., Qian, F., Zhou, C., Zhang, S., Chen, J., 2014. Preparation of magnetic porous carbon from waste hydrochar by simultaneous activation and magnetization for tetracycline removal. Bioresour. Technol., **154**, 209-214.